Multi-spatial-mode single-beam quadrature squeezed states of light from four-wave mixing in hot rubidium vapor

Neil Corzo,[1,2,*] **Alberto M. Marino,**[1] **Kevin M. Jones,**[3] **and Paul D. Lett**[1]

[1]*Joint Quantum Institute, National Institute of Standards and Technology and the University of Maryland, Gaithersburg, Maryland 20899 USA*
[2]*Departamento de Física, CINVESTAV-IPN, México D.F., 07360, Mexico*
[3]*Department of Physics, Williams College, Williamstown, Massachusetts 01267 USA*

[*]*neil.corzotrejo@nist.gov*

Abstract: We present experimental results on the generation of multi-spatial-mode, single-beam, quadrature squeezed light using four-wave mixing in hot Rb vapor. Squeezing and phase-sensitive deamplification are observed over a range of powers and detunings near the ^{85}Rb D1 atomic transition. We observe -3 dB of vacuum quadrature squeezing, comparable to the best single-spatial mode results previously reported using atomic vapors, however, produced here in multiple spatial modes. We confirm that the squeezing is present in more than one transverse mode by studying the spatial distribution of the noise properties of the field.

References and links

1. R. E. Slusher, L. W. Hollberg, B. Yurke, J. C. Mertz, and J. F. Valley, "Observation of squeezed states generated by four-wave mixing in an optical cavity," Phys. Rev. Lett. **55,** 2409–2412 (1985).
2. C. M. Caves, "Quantum-mechanical noise in an interferometer," Phys. Rev. D **23,** 1693–1708 (1981).
3. K. McKenzie, D. Shaddock, D. McClelland, B. Buchler, and P.-K. Lam, "Experimental demonstration of a squeezing-enhanced power-recycled Michelson interferometer for gravitational wave detection," Phys. Rev. Lett. **88,** 231102 (2002).
4. H. Vahlbruch, M. Mehmet, S. Chelkowski, B. Hage, A. Franzen, N. Lastzka, S. Gossler, K. Danzmann, and R. Schnabel, "Observation of squeezed light with 10 dB quantum-noise reduction," Phys. Rev. Lett. **100**, 033602 (2008)
5. T. Aoki, N. Takei, H. Yonezawa, K. Wakui, T. Hiraoka, A. Furusawa, and P. van Loock, "Experimental creation of a fully inseparable tripartite continuous-variable state," Phys. Rev. Lett. **91,** 080404 (2003).
6. A. S. Coelho, F. A. S. Barbosa, K. N. Cassemiro, A. S. Villar, M. Martinelli, and P. Nussenzveig, "Three-color entanglement," Science **326,** 823–826 (2009).
7. N. C. Menicucci, S. T. Flammina, and O. Pfister, "One-way quantum computing in the optical frequency comb," Phys. Rev. Lett. **101,** 130501 (2008).
8. A. Eckstein, and C. Silberhorn, "Broadband frequency mode entanglement in waveguided parametric downconvertion," Opt. Lett. **33,** 1825–1827 (2008).
9. B. Chalopin, F. Scazza, C. Fabre, and N. Treps,"Direct generation of a multi-transverse mode non-classical state of light," Opt. Express **19,** 4405–4410 (2011).
10. J. Janousek, K. Wagner, J. F. Morizur, N. Treps, P. K. Lam, C. C. Harb, and H. A. Bachor, "Optical entanglement of co-propagating modes," Nat. Photonics **3,** 399–402 (2009).
11. P. Kumar and M. Kolobov, "Degenerate four-wave mixing as a source for spatially-broadband squeezed light," Opt. Comm. **104,** 374–378 (1994).
12. M. Kolobov and P. Kumar, "Sub-shot-noise microscopy: imaging of faint phase objects with squeezed light," Opt. Lett. **18,** 849–851 (1993).

13. M. Vasilyev, N. Stelmakh, and P. Kumar, "Phase-sensitive image amplification with elliptical Gaussian pump," Opt. Express **17,** 11415–11425 (2009).
14. I. Sokolov and M. Kolobov, "Squeezed-light source for superresolving microscopy," Opt. Lett. **29,** 703–705 (2004).
15. L. Lopez, N. Treps, B. Chalopin, C. Fabre, and A. Maitre, "Quantum processing of images by continuous wave optical parametric amplification," Phys. Rev. Lett. **100,** 013604 (2008).
16. M. I. Kolobov, "The spatial behavior of nonclassical light," Rev. Mod. Phys. **71,** 1539–1589 (1999).
17. A. Gatti, E. Brambilla, and L. Lugiato, "Quantum Imaging," in *Progress in Optics*, E. Wolf, ed. (Elsevier, 2007), Vol. 51, p. 251.
18. M. Kolobov, ed., *Quantum Imaging* (Springer, 2007).
19. E. Lantz and F. Devaux, "Parametric amplification of images: from time gating to noiseless amplification," IEEE J. Sel. Top. Quantum Electron. **14,** 635–647 (2008).
20. M. Hosseini, B. M. Sparkes, G. Campbell, P. K. Lam, and B. C. Buchler, "High efficiency coherent optical memory with warm rubidium vapour," Nat. Commun. **2**, 174 (2011).
21. C. F. McCormick, A. M. Marino, V. Boyer, and P. D. Lett, "Strong low-frequency quantum correlations from a four-wave mixing amplifier," Phys. Rev. A **78,** 043816 (2008).
22. R. Pooser, A. Marino, V. Boyer, K. M. Jones, and P. D. Lett, "Quantum correlated light beams from non-degenerate four-wave mixing in an atomic vapor: the D1 and D2 lines of 85Rb and 87Rb," Opt. Express **17,** 16722–16730 (2009).
23. V. Boyer, A. M. Marino, and P. D. Lett, "Generation of spatially broadband twin beams for quantum imaging," Phys. Rev. Lett. **100**, 143601 (2008).
24. A. M. Marino, V. Boyer, R. C. Pooser, P. D. Lett, K. Lemons, and K. M. Jones, "Delocalized correlations in twin light beams with orbital angular momentum," Phys. Rev. Lett. **101**, 093602 (2008).
25. V. Boyer, A. M. Marino, R. C. Pooser, and P. D. Lett, "Entangled images from four-wave mixing," Science **321,** 544–547 (2008).
26. R. C. Pooser, A. M. Marino, V. Boyer, K. M. Jones, and P. D. Lett, "Low-noise amplification of a continuous-variable quantum state," Phys. Rev. Lett. **103,** 010501 (2009).
27. A. M. Marino, R. C. Pooser, V. Boyer, and P. D. Lett, "Tunable delay of Einstein–Podolsky–Rosen entanglement," Nature **457**, 859–862 (2009).
28. A. Lambrecht, T. Coudreau, A. M. Steinberg, and E. Giacobino, "Squeezing with cold atoms," Europhys. Lett. **36,** 93–98 (1996).
29. I. H. Agha, G. Messin, and P. Grangier, "Generation of pulsed and continuous-wave squeezed light with [87]Rb vapor," Opt. Express **18,** 4198–4205 (2010).
30. Note that the definitions of Δ and δ used here differ from those in Ref. [22].
31. W. V. Davis, M. Kauranen, E. M. Nagasako, R. J. Gehr, A. L. Gaeta, and R. W. Boyd, "Excess noise acquired by a laser beam after propagating through an atomic-potassium vapor," Phys. Rev. A **51,** 4152–4159 (1995).
32. K. McKenzie, E. E. Mikhailov, K. Goda, P. K. Lam, N. Grosse, M. B. Gray, N. Mavalvala, and D. E. McClelland, "Quantum noise locking," J. Opt. B **7,** S241–S428 (2005).
33. M. Martinelli, N. Treps, S. Ducci, S. Gigan, A. Matre, and C. Fabre, "Experimental study of the spatial distribution of quantum correlations in a confocal optical parametric oscillator," Phys. Rev. A **67,** 023808 (2003).
34. J. Levenson, I. Abram, T. Rivera, and P. Grangier, "Reduction of quantum noise in optical parametric amplification," J. Opt. Soc. Am. B **10,** 2233–2238 (1993).
35. S.-K. Choi, M. Vasilyev, and P. Kumar, "Noiseless optical amplification of images," Phys. Rev. Lett. **83,** 1938-1941 (1999).
36. A. Mosset, F. Devaux, and E. Lantz, "Spatially noiseless optical amplification of images," Phys. Rev. Lett. **94,** 223603 (2005).

---

1. Introduction

The generation of squeezed states of light has been a subject of research since its first experimental demonstration, using four-wave mixing (4WM) in sodium vapor, by Slusher et al. [1]. A variety of techniques for producing different types of squeezing have been explored, each with their own advantages and limitations for particular applications. For example, enhancing the precision of the optical interferometers used for gravity wave detection requires a single-beam, single-spatial-mode, quadrature squeezed state of light, with squeezing at audio frequency sidebands [2, 3]. Highly refined optical parametric oscillators (OPOs) have been developed to meet this need [4]. Continuous-variable quantum computing applications need entangled states, either produced directly in the form of squeezed twin beams or by linear optical processing of single-beam quadrature squeezed states [5]. Further, for quantum computing purposes

it is desirable to produce squeezing in multiple frequency [6–8] or spatial [9–11] modes simultaneously. Continuous-variable quantum image processing techniques have been proposed that require multi-spatial mode squeezed light or a device capable of acting as a multimode phase sensitive amplifier [12–15]. Reviews that cover continuous-variable quantum imaging include [16–19].

Techniques for producing squeezed light have been based on either parametric downconversion or 4WM in solid materials or on various wave-mixing schemes in atomic vapors. Generally speaking, techniques based on downconversion in solids have produced higher levels of squeezing. While a high level of squeezing is obviously desirable, additional considerations such as the type of squeezed state, squeezing bandwidth, and single/multi-spatial mode character of the state are considerations in evaluating the merits of different techniques for particular applications. For example, light intended to be used with an atomic-vapor-based quantum memory [20], must have the correct frequency and bandwidth to match the absorption lines of the atomic vapor, and it is thus natural for such purposes to consider atomic-vapor-based squeezing sources. Recently we have found [21, 22] that 4WM in Rb atomic vapor can produce entangled twin beams with intensity-difference squeezing levels approaching the highest quadrature squeezing levels demonstrated with downconversion crystals in an OPO. The 4WM was configured in an off-resonant double-Λ arrangement and relied on coherences between two atomic ground state levels. This arrangement reduces the excess noise that limited earlier 4WM experiments. The large non-linearity of the atomic vapor for near resonant light permits operation without a cavity. This is a very attractive feature that makes performing operations on multiple spatial modes straightforward [23–25]. In addition, the lack of a cavity simplifies applications in which light must be coupled into the system with low loss, for example when the system is used as a quantum limited amplifier [26] or as a quantum delay line [27].

Motivated by the success of the double-Λ 4WM scheme in Rb vapor for producing twin beams, we consider here the application of the same basic scheme for the production of single-beam quadrature squeezed light. We demonstrate that with proper choice of operating parameters this system can produce as much as (-3.0 ± 0.3) dB (-3.5 dB corrected for losses) of squeezing. (All uncertainties quoted in this paper are one standard deviation, combined statistical and systematic uncertainties.) Further, we show that multiple spatial modes are squeezed, making this source of interest for optical image processing. The observed squeezing level compares favorably with the highest level of single-beam squeezing obtained in atomic vapors (-2.2 dB in a cold Cs vapor [28]), and exceeds somewhat that obtained in Rb vapor specifically (-1.4 dB [29]), as well as that obtained for multi-spatial mode single-beam squeezing from an OPO with a cleverly designed self-imaging cavity (-1.2 dB [9]). We have also observed that the squeezing spectrum extends continuously to low frequencies (at least as low as 5 kHz, limited by technical noise in the present experiments).

2. Experimental setup and results

To generate twin-beam-type squeezing with a double-Λ configuration in Rb vapor we use the configuration shown in Fig. 1(a) [21,22]. A single linearly polarized pump beam, ν_p, is crossed at a small angle by an orthogonally polarized and much weaker probe beam, ν_1. The 4WM process amplifies the probe and generates a quantum-correlated conjugate beam, ν_2, on the other side of the pump. High levels of intensity difference squeezing between the probe and conjugate beams are observed when the pump beam is detuned on the order of 1 GHz to the blue of the ^{85}Rb $5S_{1/2}, F = 2 \rightarrow 5P_{1/2}$ resonance at 795 nm (outside of the Doppler-broadened absorption profile), i.e. when the one-photon detuning Δ, as defined in Fig. 1(a), is approximately 4 GHz. The probe is tuned to the red of the pump by approximately the ground state hyperfine splitting $\nu_{HF} = 3036$ MHz, and the spontaneously generated conjugate beam is approximately ν_{HF} to
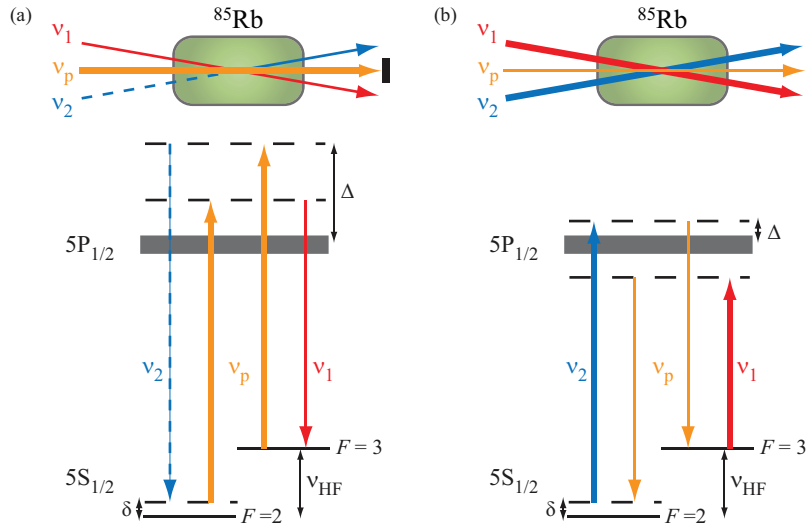
the blue of the pump.

Fig. 1. 4WM in hot ^{85}Rb vapor. (a) Twin beam generation. The top panel shows the physical arrangement of the beams in the Rb cell. The lower panel shows the level structure of the D1 transition of ^{85}Rb and the optical frequencies arranged in the double-Λ configuration. Here ν_p indicates the pump, while ν_1 and ν_2 indicate the probe and conjugate, respectively. (b) Corresponding diagrams for the generation of single-beam quadrature squeezing. Here ν_1 and ν_2 are the pumps and ν_p is the probe. For both (a) and (b): the width of the excited state in the level diagram represents the Doppler broadened line, Δ is the one-photon detuning, δ is the two-photon detuning, and ν_{HF} is the hyperfine splitting.

Our approach to generating single-beam quadrature squeezing is based on the idea of inverting this configuration as shown in Fig. 1(b). We would now like to pump with two relatively strong beams with the frequencies of, and along the directions of, the probe and conjugate beams in Fig. 1(a) and probe with a weak beam having the frequency and direction of the previous pump. Unfortunately, this simple exchange of the roles of the pump and the probe and conjugate beams does not lead to quadrature squeezing of the probe and instead we have found excess noise when the roles of the beams are simply inverted in this manner. This noise is due, at least in part, to extraneous 4WM processes. We have, however, been able to see quadrature squeezing by adjusting the operating parameters. In particular, we found it necessary to tune ν_1 and ν_2 (the two pumps) so that one is above, and the other below, the corresponding atomic resonance as shown in the energy level diagram in Fig. 1(b). In this case ν_p is blue of one resonance and red of the other, whereas in the previous configuration it was blue of both resonances. When the probe beam is injected as shown, this configuration can be viewed as a phase-sensitive amplifier for the probe beam. Using this configuration we have investigated the generation of quadrature-squeezed bright beams, obtained by deamplifying the injected probe. When the input probe beam is absent, this configuration generates squeezed vacuum and we have investigated this mode of operation as well.

In order to implement this scheme we use the experimental setup shown in Fig. 2. A Ti:Sapphire laser at frequency ν_p is tuned approximately 0.8 GHz to the blue of the ^{85}Rb $5S_{1/2}, F = 3 \rightarrow 5P_{1/2}$ transition (and hence is red of the ^{85}Rb $5S_{1/2}, F = 2 \rightarrow 5P_{1/2}$ transition, see Fig. 1(b)). The two pump frequencies are generated by frequency-shifting the light with

two double-passed 1.52 GHz acousto-optic modulators (AOMs). One beam (v_2) is upshifted by approximately v_{HF} and the other downshifted (v_1) by precisely the same amount. The AOM frequency shift, and hence the two-photon detuning $\delta = v_1 + v_{HF} - v_p$, is adjusted to optimize performance and is set to -4 MHz for all the data presented here [30]. The beams out of the AOMs (0.5 mW each) are used to seed two tapered amplifiers and thus generate two strong ($\sim$500 mW each) pump beams. The pump beams are spatially filtered with polarization-maintaining fibers and we obtained maximum powers of 230 mW and 190 mW for the beams at v_1 and v_2, respectively, when the amplifiers were at peak performance. The maximum available power varied somewhat over the course of the experiments and the values used for various data sets are indicated. The two pumps have the same linear polarization which is orthogonal to the polarization of the probe. These pump beams are directed into a 12.5 mm vapor cell filled with isotopically pure ^{85}Rb heated to 90 °C and with an angle of 0.4 degrees between the beams, as shown in Fig. 1(b). The pumps are focused with waists ($1/e^2$ radius) at the center of the cell of 600 μm. After the cell the pump light is filtered out using a Glan-Taylor polarizer and the output probe beam is sent to either a photodiode (when the process is seeded) or a homodyne detector (when the process is not seeded).
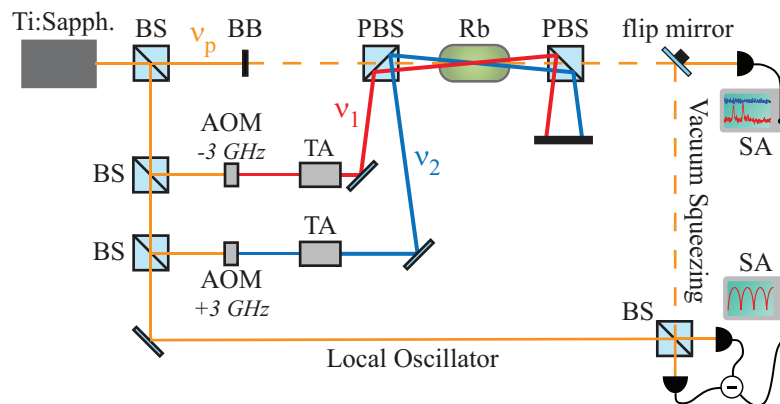

Fig. 2. Experimental setup. AOM: acousto-optic modulator, TA: semiconductor tapered amplifier, SA: radio frequency spectrum analyzer, BS: non-polarizing beamsplitter, PBS: polarizing beamsplitter, BB: beam block. The beam block and the flip mirror are removed in order to seed the 4WM process and permit direct intensity detection with a single photodiode.

We start by performing experiments in which the 4WM process is seeded and thus the system acts as a phase-sensitive amplifier (PSA) for the probe. The 4WM process can convert one photon from each of the pumps into two photons of the probe, or vice versa, depending on the phase difference between the pumps and the probe. As the phase of the probe relative to the two pumps is varied, the gain G varies between $G > 1$ (amplification) and $G < 1$ (deamplification). In particular, when the phases are set such that the input probe beam gets maximally deamplified, an ideal PSA produces an amplitude squeezed state with a squeezing level equal to G (on a linear scale). The squeezing is in the amplitude quadrature and direct detection with a single photodiode can be used to measure both the gain and the level of squeezing. To perform these measurements we remove the beam block shown in Fig. 2 and seed the process with a weak (60 μW) probe beam with a waist ($1/e^2$ radius) of 250 μm at the center of the cell where it intersects the pump beams.

Because of the phase-sensitive nature of the process, a system to lock the relative phases

of the pumps and the probe beam is required. We implement such a system by measuring the 3 GHz beat notes between each pump and the probe. We mix each of these signals down to DC using a radio frequency (RF) local oscillator derived from the signal generator which is used to drive the AOMs. This produces two error signals that are proportional to the difference in phase between each pair of beams. We then use these signals to feed back to mirrors mounted on piezoelectric crystals that control the phases of the two pumps relative to that of the probe (feedback bandwidth ≈ 1 kHz). The phase difference between the input beams can be changed with a tunable RF delay line in one of the beat note signals, making it possible to control the quadrature that is squeezed. Once this phase is adjusted such that the process gives the maximum deamplification, the gain (in this case $G < 1$) is measured by taking the ratio between the output and input probe powers. The squeezing level is measured by sending the probe to an amplified photodetector whose output is monitored by an RF spectrum analyzer. The standard quantum limit (SQL) is established by measuring the noise on a shot-noise-limited beam having the same power as the output probe. For these measurements the RF spectrum analyzer was set to a frequency of 1 MHz with a resolution bandwidth (RBW) of 30 kHz and a video bandwidth (VBW) of 100 Hz.
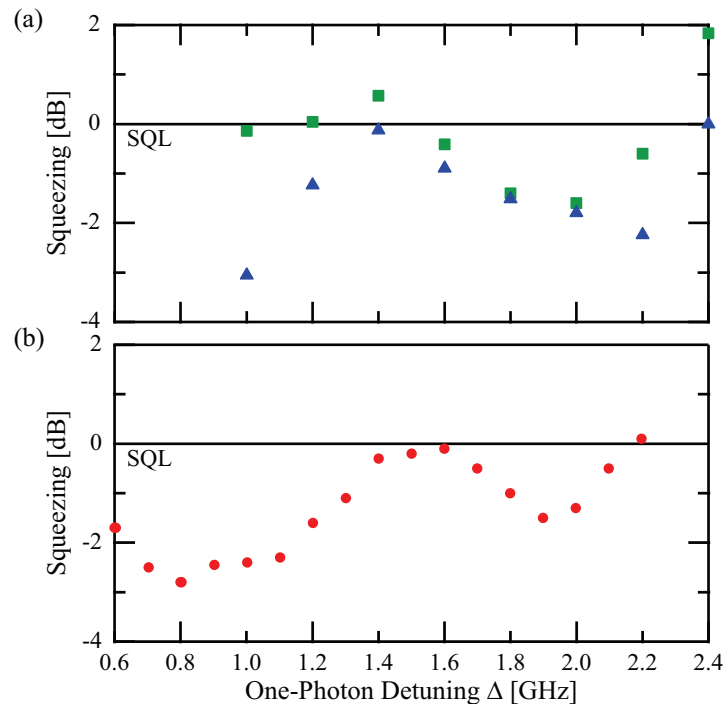

Fig. 3. Squeezing measurements at 1 MHz as a function of one photon detuning Δ. (a) (Green squares) Amplitude-quadrature squeezing measured when the 4WM process is seeded with 60 μW. (Blue triangles) The squeezing expected for an ideal PSA, calculated from the measured gain at each value of Δ, and corrected for loss. The powers in pump 1 and pump 2 are both 190 mW. (b) (Red circles) Measured squeezing when the process is not seeded (vacuum squeezing). The power in pump 1 is 230 mW, and the power in pump 2 is 160 mW. For both (a) and (b): $\delta = -4$ MHz , RBW $= 30$ kHz, VBW $= 100$ Hz.

Figure 3(a) shows the measured amplitude-quadrature squeezing (green squares) and the expected level of squeezing from an ideal PSA (blue triangles) given the measured gain of the

amplifier, all as a function of the one-photon detuning. The expected squeezing levels have been corrected for the 91 % efficiency of the direct-detection system. The measured squeezing is largest at $\Delta = 2$ GHz with a value of (-1.6 ± 0.2) dB. In the region $\Delta = 1.4$ GHz to 2.0 GHz, the observed squeezing is close to that expected for an ideal PSA. For values of Δ outside of this range the measured squeezing is less than that expected for an ideal system, indicating the presence of some additional noise process. When $\Delta = 0$ or $\Delta = 3.0$ GHz the probe (ν_p) is tuned to an atomic resonance (see Fig. 1(b)). The squeezing degrades as ν_p approaches either resonance, suggesting that the additional noise is, at least in part, associated with having this beam tuned near resonance. The gain, and thus the expected level of squeezing, disappears at one-photon detunings around 1.4 GHz. That the gain is minimized between the atomic resonances is to be expected when the contributions to the $\chi^{(3)}$ from the two resonances are summed.

Early on in these experiments we observed additional beams exiting from the cell under some conditions. From the directions and behavior of these "extra" beams we infer that they are due to unintended 4WM processes like the ones used to generate twin beams (see Fig. 1(a)), i.e., processes which involve the probe beam interacting with only one pump and which thus generate an additional conjugate beam on the other side of that pump. Since these extra 4WM processes are independent of the phase-sensitive one that we are interested in driving, they add uncorrelated noise to the probe beam and limit the amount of squeezing that can be obtained. We were originally led to the one photon detuning range used above by searching for a detuning which minimized these competing 4WM processes. Only by doing so were we able to observe squeezing. As noted earlier, this detuning range is different from that used for generating twin-beam squeezing (see Fig. 1), for which $\Delta \approx 3.8$ GHz is typical and no squeezing has been observed for Δ below 3 GHz.

In addition to the 4WM processes that generate visible "extra" beams, less obvious single-beam 4WM processes can add noise as well. Davis et al. [31] have shown that a single beam propagating through an atomic vapor and tuned near an atomic resonance will acquire excess noise, with the level of this noise depending on the power and detuning of the beam. They attribute this to a forward 4WM process between the carrier and its sidebands. This process amplifies the sidebands which are initially in a vacuum state, leading to excess noise. In our case this would result in a degradation of the levels of squeezing when the probe is tuned near the atomic resonances, as observed. Davis et al. [31] noted an asymmetry in the noise on the two sides of the atomic line. We repeated their experiment for our system and parameters and found that the excess noise blue of the lower ($\Delta = 0$ GHz) atomic line extends further in detuning than the noise red of the higher ($\Delta = 3.0$ GHz) line. This is consistent with our observation that the detuning region where squeezing is observed lies closer to the higher line than the lower line. Since this single beam excess noise is due to mixing of the carrier and sidebands of the probe, it should be possible to largely avoid this unwanted effect by working with a squeezed vacuum probe rather than a bright probe beam. We now explore that idea.

If we do not seed the 4WM process (i.e., if we insert the beam block in Fig. 2) the probe field grows from vacuum and the system generates a squeezed vacuum state. Since the number of generated photons is low we use a homodyne detection scheme to measure the squeezing level. For the local oscillator (LO) we use a portion of the Ti:Sapphire laser at ν_p. The phase of the LO relative to that of the squeezed vacuum beam is scanned by using a mirror mounted on a piezoelectric crystal, thus selecting different quadratures of the squeezed state. An RF spectrum analyzer is then used to measure the noise level of the signal from the homodyne detector. Figure 4(a) shows the noise level as the phase of the LO is scanned. The settings of the spectrum analyzer are the same as the ones used above.

To obtain an accurate measure of the vacuum squeezing level as a function of different experimental parameters, we implement a feedback system to lock the phase of the LO to the
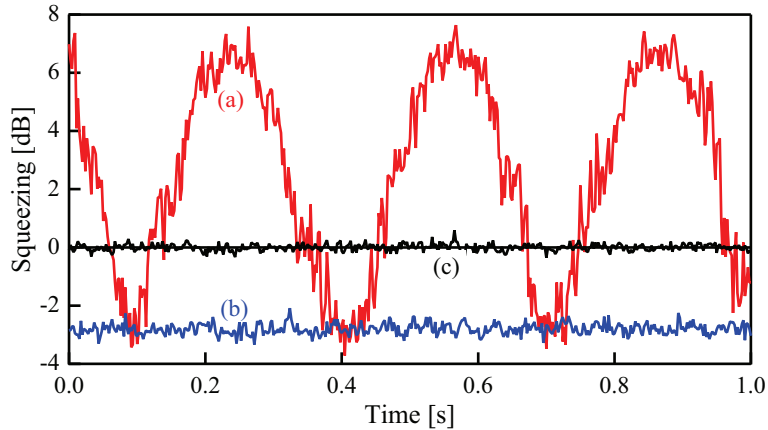
Fig. 4. Vacuum squeezing measured by homodyne detection at 1 MHz when (a) the phase of the local oscillator (LO) is scanned and (b) when the phase of the LO is locked. Trace (c) indicates the standard quantum limit. (RBW = 30 kHz, VBW = 100 Hz.) Comparison of the traces shows a squeezing level of (-2.8 ± 0.2) dB. Here $\Delta = 0.8$ GHz, $\delta = -4$ MHz, the power in pump 1 is 230 mW and the power in pump 2 is 160 mW.

phase of the vacuum squeezed state. Following ref. [32], where this "quantum noise locking" technique is described in detail, the phase of the squeezed beam is modulated at 5 kHz. This leads to a modulation of the noise power signal measured at 1 MHz. The noise power is then demodulated to produce an error signal which has zero crossings at the minimum and maximum noise levels, making it possible to lock at either of these noise levels. Figure 4(b) shows the noise level with the locking system operational. The noise level remains constant at a level of (-2.8 ± 0.2) dB of squeezing. Taking into account the overall homodyne detection efficiency of 89 % the inferred level of squeezing coming out of the source is -3.3 dB. With the LO locking turned off, and the LO phase sweeping, the measured squeezing level on a trace can be -3.0 dB or slightly better, suggesting that the source is capable of producing at least -3.5 dB of squeezing.

Figure 3(b) shows the vacuum squeezing as a function of the one-photon detuning Δ. In addition to observing squeezing at detunings near 2.0 GHz, as in the case of the seeded process, squeezing is also present in a region centered around 0.8 GHz. This suggests that the single-beam 4WM process of [31] was indeed a limiting factor in the seeded measurements presented in Fig. 3(a). From Fig. 3 it is apparent that vacuum squeezing is obtained over a larger detuning range, and results in higher levels of squeezing than can be obtained with the seeded process. In any case, the levels of noise reduction obtained in the single-beam configuration (Fig. 1(b)) explored here are significantly lower than those obtained for the twin-beam configuration (Fig. 1(a)) in the same double-Λ system [21, 22].

In addition we have examined the dependance of the vacuum squeezing on the pump powers. In performing these measurements we have used the same detunings as were used in Fig. 4 (which were optimized for the maximum pump powers available). As shown in Fig. 5, squeezing is present over a large range of powers, even as low as 25 mW in each pump beam. The best results are obtained at higher pump powers, but we see a saturation in the squeezing level with pump power, suggesting that higher pump powers will not increase the squeezing level much beyond what has been observed here. We have also explored varying the temperature of the cell and found the optimum was approximately 90 °C. Increasing the temperature beyond

this point increases the gain of all of the competing 4WM processes, as well as the absorption in the Doppler-broadened medium, in such a way as to reduce the measured level of squeezing.
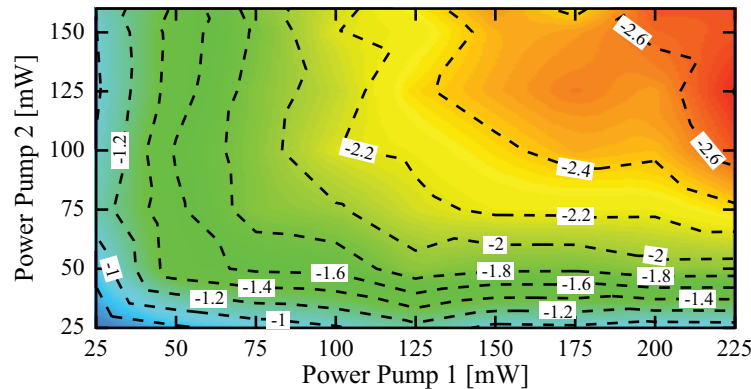

Fig. 5. Measured vacuum squeezing at 1 MHZ (RBW = 30 kHz, VBW = 100 kHz) as a function of pump powers. The contour lines give the squeezing in decibels. $\Delta = 0.8$ GHz, $\delta = -4$ MHz.

The noise measurements discussed above were all taken at an analysis frequency of 1 MHz. We have explored the variation in squeezing with the choice of analysis frequency. At the low end we find the squeezing level to be constant down to frequencies where the technical noise dominates, about 5 kHz with the present apparatus. At the high end, with the parameters used for these measurements, squeezing extends up to approximately 10 MHz, however, this depends strongly on the two-photon detuning δ and weakly on the pump power. A study of these effects will be presented elsewhere.

3. Multimode behavior

One of the most important and distinctive properties of our source of single-beam quadrature-squeezed light is its multi-spatial-mode character. Generating a multi-spatial-mode squeezed state has been a goal of a number of other studies [9–11] and would enable certain approaches to enhancing resolution in optical imaging systems [12, 14, 18]. A study of the spatial distribution of the noise in the squeezed beam provides a method to distinguish between single and multiple spatial modes. For a single-spatial-mode squeezed state, any loss mechanism, independent of its origin, behaves just as an attenuation. Thus, even if the losses are due to spatial masking of the beam, the level of squeezing (on a linear scale) is attenuated linearly with the loss towards a vacuum state (the SQL). On the other hand, for a multi-spatial-mode squeezed beam there can be a dependence of the noise properties on the spatial variation of the loss, since different regions of the beam are independent of each other. Such a difference in the behavior of the squeezing as a function of spatially varying losses provides a method to distinguish between single and multi-spatial mode character [33]. That is, if the level of squeezing as a function of the attenuation deviates from a straight line it is a signature of the multi-spatial-mode nature of the beam.

We implement three measurements that involve different spatial masking of the squeezed beam. In order to perform the masking we block parts of the LO beam rather than masking the squeezed beam directly. If one were to perform the masking by directly blocking the squeezed beam it would be necessary to modify the shape of the LO as well in order to maintain the mode matching between the squeezed beam after the mask and the LO in the homodyne detection.
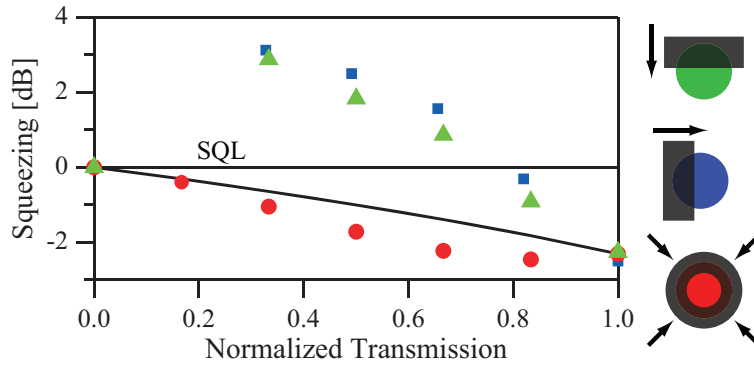
Fig. 6. Vacuum squeezing measured at 1 MHz (RBW = 10 kHz, VBW = 300 Hz) for different forms of spatially-dependent losses. We show the behavior of the vacuum squeezing when we cut the LO with an iris (red circles), or with a razor blade from the top (green triangles) and from the side (blue squares). The uncertainties in the squeezing measurements are approximately the size of the symbols. We also show the expected behavior of a single-mode squeezed beam (black curve). Here $\Delta = 0.8$ GHz, $\delta = -4$ MHz. The power in pump 1 is 230 mW, and in pump 2 is 160 mW.

(Failing to do so would imply measuring part of a vacuum mode in addition to the desired squeezed mode.) On the other hand, when performing a homodyne detection, the shape of the LO can effectively act as a spatial filter or mask that selects out the shape of the beam that is being measured. Thus by cutting the LO beam we effectively mask the squeezed beam and the LO simultaneously and avoid introducing any extra vacuum noise that would result from the reduction of the mode matching efficiency described above. The results are shown in Fig. 6, where we plot the squeezing as a function of transmission when we cut the LO beam radially with an iris (red circles), with a razor blade from the top (green triangles), or with a razor blade from the side (blue squares). We also plot the expected behavior of a single-spatial-mode squeezed beam as a function of the losses (black curve); in this case, as described above, the expected behavior is linear (note that Fig. 6 is plotted on a logarithmic scale). The three different methods of cutting the beam all deviate from the expected linear behavior characteristic of a single-spatial-mode beam. This difference is the signature of the multi-spatial-mode nature of the output from the 4WM process.

We can get an idea of the number of modes in the region measured by the homodyne detection by calculating the number of coherence areas that fit within the detection area, which is determined by the size of the LO. The coherence area is the smallest independent region in the transverse profile of the squeezed beam and thus gives an indication of the smallest resolvable region. A rough estimate of the size of the coherence area can be obtained from the behavior of the vacuum squeezing when the LO is cut with an iris (red circles in Fig. 6). Once the size of the iris reaches the size of the coherence area the field behaves as a single mode and thus the squeezing level should start to decrease linearly with transmission. This behavior is not apparent in Fig. 6, thus we use the point at a transmission around 0.15 as an upper bound for when the size of the iris reaches the size of the coherence area. Given the Gaussian spatial profile of the LO, such a transmission level corresponds to 8 % of its area. Thus, we can estimate that there are at least 12 modes inside the detection region. Note that squeezed light may be generated over a larger area than the full LO detection region, and thus this is a lower limit on the number of squeezed modes that are generated. An accurate measure of the number of modes

would require measuring the spatial bandwidth in addition to the size of the coherence area, as was done in [23] for twin beams. A more in-depth study of the multi-spatial mode properties of the system will be presented elsewhere.

From Fig. 6 we can also see that there is a clear difference in how the noise scales with losses when the beam is cut in different ways. In addition, there is almost no difference between the use of a razor blade to cut from the top or from the side of the beam. In both cases the squeezing is lost very rapidly. The difference comes when we use the iris to mask the beam. In this case there is always squeezing and it always has lower noise than would be obtained if one were attenuating a single-spatial-mode squeezed beam by the same amount. The symmetric behavior of the noise with respect to the center of the probe can be explained by the phase matching conditions of the 4WM process. When a photon from each of the pump beams is absorbed in order to generate two photons in the probe beam momentum conservation (see Fig. 1(b)) only requires that the two photons of the probe are created in such a way that the total momentum perpendicular to the propagation axis of the probe is zero, leading to a symmetry around the axis.

4. Conclusion

We have demonstrated that 4WM in ^{85}Rb vapor in a double-Λ configuration can generate multi-spatial mode single-beam vacuum quadrature-squeezed light with a squeezing level of up to (-3.0 ± 0.3) dB. Using the same double-Λ system as the one used in [21] to generate twin beams, we are able to overcome, with the help of the ground state coherences and relatively large detunings, spontaneous emission and absorption problems present in a number of previous experiments based on 4WM in atomic systems. For our experimental configuration the main limitation to the amount of squeezing that can be obtained is the competition with other 4WM processes that introduce extra noise on the squeezed beam. These competing processes include the phase-insensitive 4WM processes between the probe and one or the other of the two pumps present, which generate additional conjugate beams on the other side of the pump from the probe, as well as single-beam 4WM processes that mix the carrier and sidebands of a bright probe beam. These processes limit the amount of noise reduction that can be obtained with the double-Λ configuration to levels lower than the ones that can be achieved in the generation of twin beams. Inasmuch as the generation of vacuum squeezing does not generate a bright probe beam, the single-beam 4WM process that generates extra noise is not a significant factor in this case. This leads to better squeezing levels for the vacuum-seeded case than for the bright-beam seeded case. In addition to the vacuum squeezing results, we have found experimental conditions where our phase-sensitive amplifier can generate bright-beam amplitude-quadrature squeezing up to a value of (-1.6 ± 0.2) dB.

We find that the generation of squeezed light with this process is relatively robust with respect to changes in the power of the pump beams. Squeezing is observed for a wide range of pump powers; even at powers as low as 25 mW in each pump beam. We have found experimental parameters where squeezing is present for analysis frequencies as low as 5 kHz, and up to 10 MHz. Squeezing is present for different one-photon detunings near the D1 line of ^{85}Rb. From previous experiments exploring twin-beam squeezing [22] we can anticipate that these results can be extended to the D1 lines of other alkalis, as well as (with more limited success) to the D2 lines of other alkalis. In order to further enhance the squeezing it is possible that one could cascade several low-gain stages, suppressing the build-up of parasitic 4WM processes between the stages, and effectively enabling one to obtain a higher gain. Such experiments should be feasible with current technology.

Finally, we have verified the multi-spatial mode nature of the squeezed beam by studying the behavior of the noise reduction as a function of spatially-varying losses. Such measurements

have made it possible for us to determine that squeezing is present in at least 12 transverse modes of the beam, making our system one of the first devices to simultaneously generate a number of single-beam squeezed transverse spatial modes [9, 10]. Such a multi-spatial mode behavior is possible due to the high gain in the medium, which permits single-pass operation and does not require a cavity, which would filter the spatial mode, to build up the field.

In the future, we will investigate the noise figure of the PSA when it is used to amplify signals. In principle, the PSA should preserve the signal-to-noise ratio of the input signal [34–36] in contrast to a phase-insensitive amplifier [26], which always leads to excess noise in the amplification process. Due to the multi-spatial-mode character of the PSA, by using this same process we should be able to implement a noiseless image amplifier. The type of multi-spatial-mode source of vacuum squeezing demonstrated here could enable the exploration of quantum imaging techniques that have been suggested but not yet demonstrated experimentally [12, 14, 16–19].

Acknowledgments